Received: 4 December 2020 | Revised: 24 February 2021 | Accepted: 8 March 2021

DOI: 10.1096/fj.202002615RR

RESEARCH ARTICLE

THE FASEB JOURNAL

Low abundance of Mfn2 protein correlates with reduced mitochondria-SR juxtaposition and mitochondrial cristae density in human men skeletal muscle: Examining organelle measurements from TEM images

Mauricio Castro-Sepulveda[1,2] | **Rodrigo Fernández-Verdejo**[3] | **Mauro Tuñón-Suárez**[1] | **Jorge Morales-Zúñiga**[4] | **Mayarling Troncoso**[5] | **Sebastian Jannas-Vela**[1] | **Hermann Zbinden-Foncea**[1,6]

[1]Escuela de Kinesiología, Facultad de Medicina, Universidad Finis Terrae, Santiago, Chile

[2]Facultad de Medicina, Pontificia Universidad Católica de Chile, Santiago, Chile

[3]Carrera de Nutrición y Dietética, Departamento de Ciencias de la Salud, Facultad de Medicina, Pontificia Universidad Católica de Chile, Santiago, Chile

[4]Laboratorio de Ciencias del Deporte, Clínica Sports Medicina Deportiva, Viña del Mar, Chile

[5]Faculty of Chemical and Pharmaceutical Science & Faculty of Medicine, Advanced Center for Chronic Diseases (ACCDiS), Universidad de Chile, Santiago, Chile

[6]Centro de Salud Deportiva, Clinica Santa Maria, Santiago, Chile

Correspondence
Mauricio Castro-Sepulveda and Hermann Zbinden-Foncea, Escuela de Kinesiologia, Facultad de Medicina, Universidad Finis Terrae, Santiago, Chile. Av. Pedro de Valdivia 1509, Providencia, Chile.
Email: (M. C.-S.) and hzbinden@uft.cl (H. Z.-F.)

Funding information
This study was funded by Research Grant awarded to MCS by Universidad Finis Terrae (Grant no. CAI 2019)

Abstract

The role of mitofusin 2 (Mfn2) in the regulation of skeletal muscle (SM) mitochondria-sarcoplasmic (SR) juxtaposition, mitochondrial morphology, mitochondrial cristae density (MCD), and SM quality has not been studied in humans. In in vitro studies, whether Mfn2 increases or decreases mitochondria-SR juxtaposition remains controversial. Transmission electron microscopy (TEM) images are commonly used to measure the organelle juxtaposition, but the measurements are performed "by-hand," thus potentially leading to between-rater differences. The purposes of this study were to: (1) examine the repeatability and reproducibility of mitochondrial-SR juxtaposition measurement from TEM images of human SM between three raters with different experience and (2) compare the mitochondrial-SR juxtaposition, mitochondrial morphology, MCD (stereological-method), and SM quality (cross-sectional area [CSA] and the maximum voluntary contraction [MVC]) between subjects with high abundance (Mfn2-HA; n = 6) and low abundance (Mfn2-LA; n = 6) of Mfn2 protein. The mitochondria-SR juxtaposition had moderate repeatability and reproducibility, with the most experienced raters showing the best values. There were no differences between Mfn2-HA and Mfn2-LA groups in mitochondrial size, distance from mitochondria to SR, CSA, or MVC. Nevertheless, the Mfn2-LA group showed lower

Abbreviations: CSA, cross-sectional area; CV, coefficients of variability; ICC, intraclass correlation coefficients; MCD, mitochondrial cristae density; Mfn, mitofusin; MVC, maximum voluntary contraction; OMM, outer mitochondrial membrane; SM, skeletal muscle; SR, sarcoplasmic reticulum; TEM, transmission electron microscopy.

mitochondria-SR interaction, MCD, and VO_{2max}. In conclusion, mitochondrial-SR juxtaposition measurement depends on the experience of the rater, and Mfn2 protein seems to play a role in the metabolic control of human men SM, by regulating the mitochondria-SR interaction.

KEYWORDS

MICOS complex, mitochondria dynamics, organelle communication, repeatability, reproducibility, transmission electron microscopy

1 | INTRODUCTION

Mitochondria are dynamic organelles that are constantly remodeling through fusion and fission events. Certain mitochondria are in close contact with other organelles, including the endo/sarcoplasmic reticulum (ER-SR).[1,2] The communication between mitochondria and ER/SR regulates diverse metabolic processes including phospholipid and calcium transfer, ROS signaling, autophagy, and mitochondrial DNA synthesis.[1-3] Over 60 proteins support the mitochondrial-ER interaction,[1-3] of which recent attention has been directed to mitofusin 2 (Mfn2), a mitochondrial profusion protein located mostly on the outer mitochondrial membrane (OMM), but also having a small fraction in ER/SR membranes.[4-6] Mfn2 mediates the mitochondria-ER/SR interactions by tethering the ER/SR to the OMM,[4,5] thus affecting the mitochondrial bioenergetic parameters such as mitochondrial cristae density (MCD).[7]

In skeletal muscle (SM), decreases in Mfn2 abundance have been related to metabolic disturbances. Mice with a SM deletion of Mfn2 show impaired mitochondrial morphology, localization, and calcium uptake,[8] resulting in decreased SM cross-sectional area [CSA] and strength.[9] In human primary myotubes, Mfn2 deletion results in decreased mitochondria-SR interaction and insulin-mediated glucose uptake.[10] Similarly, we have recently shown that the ratio of Mfn2/Fis1 (Fis1 [fission 1]) associates directly with the whole-body relative lipid oxidation.[11] Together, this evidence suggests that Mfn2 has a central role in the regulation of SM metabolism by controlling the mitochondria-SR interaction. Nevertheless, this hypothesis has not been tested in humans.

Despite the evidence on the role of Mfn2 in the regulation of mitochondria-ER/SR juxtaposition (ie, distance and interaction between organelles), its exact function in this inter-organelle interplay (decrease or increase membrane juxtaposition) still remains a matter of intense debate.[12,13] Differences in the models for Mfn2 ablation or in the culture media, as well as different silencing efficiency, could explain the controversies observed in cell studies. Besides, two types of contact sites between mitochondria-ER have been recently demonstrated, that is, narrow (8-10 nm) and wide (40-50 nm).[14] An acute Mfn2 downregulation was shown to increase the number of narrow contacts by ≈40%, but to decrease the number of wide contacts by ≈30%.[14] This differential response may explain the controversy regarding the exact role of Mfn2 in the regulation of mitochondria-ER/SR juxtaposition. Additionally, issues in the repeatability and reproducibility of measurements may also be involved, since they are performed "by hand," and therefore, could yield discrepancies between raters. The most common protocol to measure the mitochondria-ER/SR juxtaposition is using transmission electron microscopy (TEM) images. First, the regions in which ER/SR and the OMM are ≤50 nm away from each other are identified. Subsequently, two aspects within this region are quantified: (1) the distance from mitochondria to SR [in nm] and (2) the length of the mitochondrial interface covered by the SR (ie, mitochondria-SR interaction [in %]).[11,15,16] To date, the repeatability (ie, intra-rater) and reproducibility (inter-rater) in the measurement of mitochondria-SR juxtaposition have not been tested.

Our current study aimed to: (1) examine the repeatability and reproducibility of mitochondrial-SR juxtaposition measurement from TEM images of human SM between three raters with different experience and (2) compare the mitochondrial-SR juxtaposition, mitochondrial morphology, MCD, and SM quality between subjects with high abundance and low abundance of Mfn2 protein in SM.

2 | MATERIALS AND METHODS

We analyzed a new subset of data from a previous study of our group.[11] The western blotting data for Mfn1-2, Opa1, and GAPDH has been previously published,[11] but herein we reanalyzed those data differently.

2.1 | Subjects

Twelve nondiabetic, nonsmoking men, without history of cardiovascular, respiratory, or thyroid disease, were included. After a 12-h fast, subjects underwent a biopsy from the *Vastus Lateralis* muscle of the dominant leg. The biopsy was split into three pieces: (1) immediately frozen in liquid nitrogen and stored at 80°C for Western blotting, (2) fixed

in 2.5% glutaraldehyde for TEM analyses, and (3) immediately frozen in cooled isopentane and stored at 80°C for hematoxylin/eosin staining. The participants were advised to maintain their usual diet, without changing the size and type of servings, and refrain from exercise 48 hours before the metabolic measurements and biopsies. All subjects signed a written informed consent approved by the Institutional Review Board at the Universidad Finis Terrae and adhered to the Declaration of Helsinki.

2.2 | Repeatability and reproducibility of mitochondrial size and mitochondrial-SR juxtaposition

2.2.1 | Preparation for TEM analyses

The SM biopsies were fixed in a glutaraldehyde solution (2.5%, room temperature, 2 hours). Fixed muscle was dissected into bundles of fibers, washed four times with 0.1 M sodium cacodylate buffer, and stained with 2% osmium tetroxide in 0.1 M sodium cacodylate buffer for 2 hours. The samples were then washed with water, stained with 1% uranyl acetate for 2 hours, dehydrated on acetone dilution series, and embedded in Epon resin. Finally, 80-nm sections were cut, mounted on grids, and examined using a TEM (Tecnai T12 at 80 kV, Philips; Microscopy Facility, Pontificia Universidad Católica de Chile). All the samples were prepared the same way by the same researcher.

2.2.2 | Images and raters' characteristics

Two to three TEM images per biopsy were captured for each subject, obtaining 34 TEM images in total. Mitochondrial size and mitochondria-SR juxtaposition were measured by three raters independently. Rater 1 had 4 years of experience in analyses of SM TEM images, rater 2 had 6 months of experience in analyses of mice brown adipose tissue from TEM images, and rater 3 was unexperienced in the analysis of TEM images. Before measurements, rater 1 trained the other raters using four TEM images of human SM. Then, each rater independently conducted each measurement twice, with at least a 2-week gap.

2.2.3 | TEM image analyses

For mitochondrial morphology, a mask was drawn over the outer membrane of the mitochondria at ×25 000 magnification (Figure 1A), as described.[11,15] The mitochondria-SR juxtaposition was analyzed when both organelles were ≤50 nm away from each other.[11,15,16] Mitochondria-SR juxtaposition had two components. First, the distance from mitochondria to SR, considered as the average of three distance readings evenly distributed over the interface between organelles (Figure 1B). Second, mitochondria-SR interaction, considered as the percentage of the mitochondrial interface covered by the SR (Figure 1C).[11,15,16] TEM images were analyzed on longitudinal sections using Fiji/ImageJ software.

2.3 | Role of Mfn2 protein on mitochondrial morphology, mitochondrial-SR juxtaposition, MCD, and SM quality

2.3.1 | Western blotting

Muscle biopsies were homogenized using an electric homogenizer in buffer containing: 20 mM of Tris-HCl (pH 7.5), 1% of Triton X-100, 2 mM of EDTA, 20 mM of NaF, 1 mM of $Na_2P_2O_7$, 10% of glycerol, 150 mM of NaCl, 10 mM of Na_3VO_4, 1 mM of PMSF, and a protease inhibitor cocktail (complete mini; Roche Applied Science). Proteins were separated by SDS-PAGE and transferred to PVDF membranes, as previously described.[11] The following antibodies (dilutions) were used: Mfn1 (1:1000, sc-166644, Santa Cruz Biotechnology), Mfn2 (1:1000, ab56889, Abcam), Opa1 (1:1000, 612606, BD Biosciences), Total OXPHOS cocktail (1:1000, ab110413, Abcam), MIC60 (1:1000, 10179-1-AP, Proteintech), and Mic19 (1:1000, 25625-1-AP, Proteintech). GAPDH (1:10 000, 2118, Cell Signaling Technology) was used as loading control.[11] Protein bands were visualized on a film (WESTAR SUPERNOVA detection kit, Cyanagen, Bologna, Italy), scanned, and quantified by densitometry using Image Lab Software Version 6.0 (Bio-Rad).

2.3.2 | MCD, stereological method

One external blinded rater estimated the MCD (%) per mitochondria volume—using standard stereological methods [17]—from 36 random fibers from each of the 12 individuals. Only mitochondrial profiles with clearly visible mitochondria were included.[17] A minimum of eight mitochondria per fiber (three fibers per subjects) were analyzed.[17]

2.3.3 | Fiber-type assessment from TEM images

Fiber type was assessed from TEM images by two parameters: (1) mitochondrial density, defined as the area of the sarcoplasm covered by mitochondria[11,16] and (2) the width of the Z-lines.[18] TEM images were measured in three separate fibers per subject on longitudinal sections using Fiji/ImageJ software.

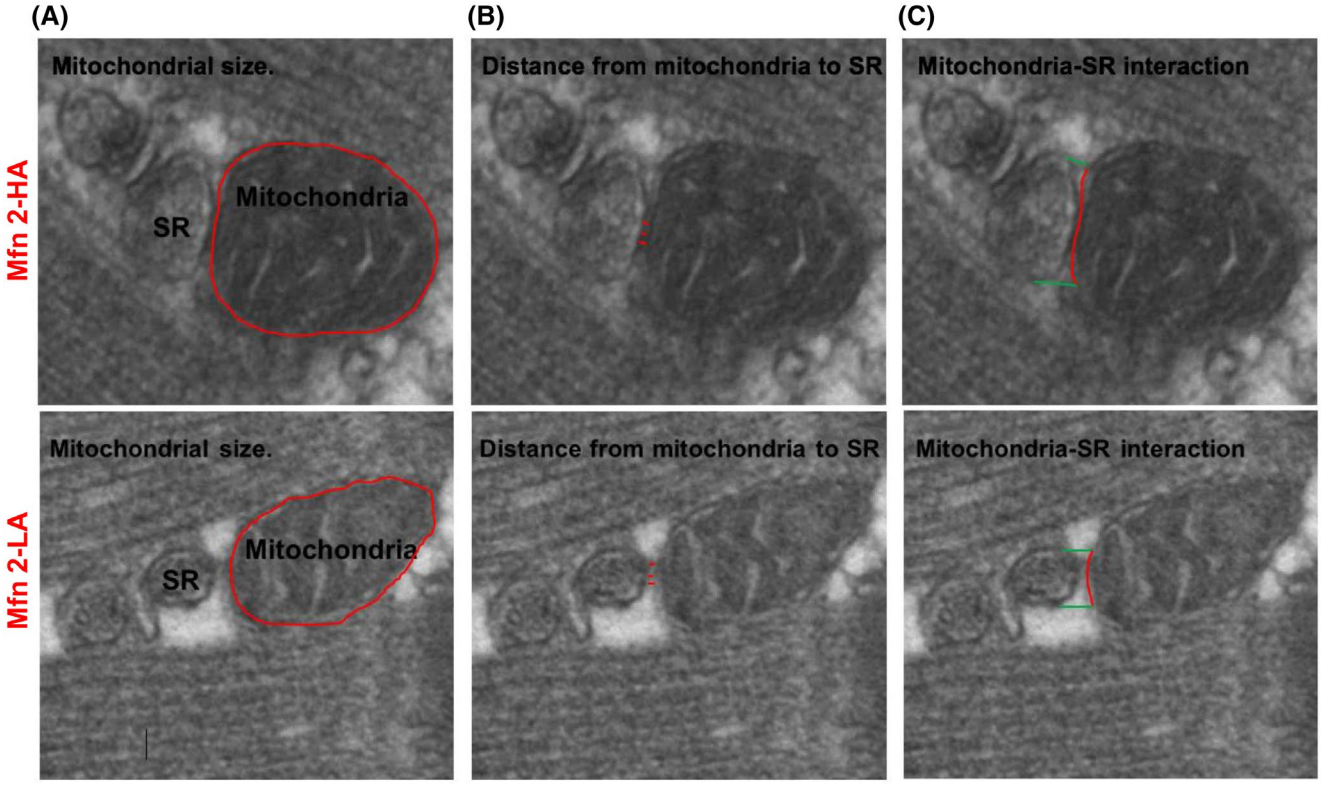

FIGURE 1 Morphometric analyses of mitochondrial size and mitochondria-SR juxtaposition from TEM images of human skeletal muscle. Representative images of mitochondrial size (A), distance from mitochondria to SR (B) and mitochondria-SR interaction (C) in human SM with Mfn 2-HA and Mfn 2-LA. SR, sarcoplasmic reticulum; TEM, transition electron microscopy; SM, skeletal muscle; Mfn 2-HA, Mfn2-high abundance; Mfn 2-LA, Mfn2-low abundance

2.3.4 | Histology

A piece (~50 mg) of the muscle biopsy was immediately frozen in cold isopentane and stored at −80°C. Cryosections (10 μm) of muscles were stained following standard protocols. CSA was quantified in ~70 fibers/volunteer using Fiji/ImageJ software.

2.3.5 | Muscle strength

MVC of the knee extensor muscles was determined in the dominant leg ~7 days before the muscle biopsy. A force plate (Tesys 1000; Globus System, Miami, FL, USA) was attached to the footplate of a leg press machine.[19] Isometric contractions were performed with the knee at 90º. Before maximal testing, subjects warmed-up by performing three submaximal isometric knee extensions (50, 70, and 80% of self-perceived MVC; 30 seconds of rest between contractions). Then, subjects performed three maximal 3-s contractions (1 minute rest between contractions), and the highest force recorded was considered as the MVC.[19]

2.3.6 | Maximum oxygen uptake

Maximum oxygen uptake (VO_{2max}) was determined during an incremental cycle ergometer test until exhaustion (8 km/hr initial workload, increases of 1 km/h each 1 minute). Before each test, the gas analyzer was calibrated with gases of known concentrations ($O_2 = 16\%$ and $CO_2 = 4\%$), and the airflow was calibrated with a 3-liter syringe (Hans Rudolph). Gas exchange was continuously measured with a breath-by-breath gas analyzer system (Ergocard; Medisoft). Subjects were considered to reach VO_{2max} when two of the following criteria were met: (1) plateau in VO_2 despite increases in workload and (2) respiratory quotient ($RQ = VCO_2/VO_2$) > 1.10; or 3) maximal estimated heart rate by the formula [220—age in years].

2.3.7 | Blood analyses

Blood serum was used to determine the insulin concentrations by chemiluminescence. Serum concentrations of triglycerides, total cholesterol, low-density lipoprotein cholesterol (LDL-C), and high-density lipoprotein cholesterol (HDL-C) were determined by dry chemistry (Bionet, Santiago, Chile). Blood samples were withdrawn ~7 days before the muscle biopsy.

2.3.8 | Statistics

Data are presented as means [standard deviations]. Repeatability (within raters) and reproducibility (between

raters) were determined with IBM® SPSS® Statistics version 26. Repeatability was assessed by repeatability coefficients (ie, the value within which two readings will be for 95% of cases),[20] intraclass correlation coefficients (ICC; two-way mixed effects, single measurement, absolute agreement),[21] and coefficients of variability (CV). Reproducibility was assessed by the limits of agreement method (corrected for repeatability, including linear regression analyses),[20] ICCs (two-way random effects, single rater, absolute agreement),[21] and CVs. Further analyses were performed using Prism 7.0 (GraphPad Software, La Jolla, CA, USA). Comparisons between Mfn2-HA and LA group were performed with an unpaired Mann-Whitney test. Correlations between Mfn2 and mitochondria-SR interaction and MCD were assessed with the Spearman test. $P < .05$ was considered significant.

3 | RESULTS

3.1 | Repeatability in the measurement of mitochondrial morphology and mitochondrial-SR juxtaposition

Supporting Information Figure S1 shows the repeated measurements of mitochondrial size (Supporting Information Figure S1A-C), distance from mitochondria to SR (Supporting Information Figure S1D-F), and mitochondria-SR interaction (Supporting Information Figure S1G-I) conducted by each rater. Table 1 summarizes the repeatability analyses. For mitochondrial size, the repeatability coefficient was, in the worst case, 84.14 nm. All raters had ICCs higher than 0.90 and CVs lower than 5%, indicating excellent repeatability.[21] A lower repeatability was observed for the measurement of mitochondria-SR juxtaposition. Repeatability coefficients were, at worst, 8.64 nm (distance) and 5.92% (interaction), with moderate-to-excellent ICCs according to their 95% confidence intervals.[21] CVs reached up to 17.5% for the distance between organelles, and 6.8% for their interaction. Of note, rater 3—that is, the less experienced—had the worst values in all the repeatability indexes. The images that generated the larger differences between repeated measurements were identified; those images are presented in Supporting Information Figure S1J-L, and their values denoted with an arrow in Supporting Information Figure S1A-I.

3.2 | Reproducibility in the measurement of mitochondrial morphology and mitochondrial-SR juxtaposition

Supporting Information Figure S2 shows Bland-Altman plots comparing the measurements between raters of mitochondrial size (Supporting Information Figure S2A-C), distance from mitochondria to SR (Supporting Information Figure S2D-F), and mitochondria-SR interaction (Supporting Information Figure S2D-I). Table 2 summarizes the reproducibility analyses. For mitochondrial size, the largest bias was 72.07 nm, and the wider limits of agreement spread over 257 nm. Linear regression analyses showed slopes not different from zero; thus, the bias was unrelated to the magnitude of the measurement. For the comparison rater 3 vs 2, the intercept of the regression was different from zero, indicating that rater 3 consistently measured 47.96 nm less than rater 2. ICCs for rater 3 vs raters 1 or 2, were high-to-excellent, as shown by their 95% confidence intervals[21]; however, the comparison rater 2 vs 1, showed a wide range, from poor-to-excellent values. Despite these differences, the CVs were lower than 5% for all comparisons.

For the distance from mitochondria to SR, the largest bias was 4.27 nm, and the limits of agreement spread over ~26 nm. In the case of mitochondrial-SR interaction, the largest bias was 3.48%, and the limits of agreement spread over ~16%. The

TABLE 1 Repeatability of the measurements

		Repeatability coefficient		Intraclass correlation		CV (%)	
Variables	**Rater**	**Absolute**	**Relative**	**Coefficient**	**95% CI**	**Mean**	**SD**
Mitochondrial size (nm)	1	56.67	1.00 [ref]	0.994	0.986 to 0.997	1.2	1.2
	2	84.14	1.48	0.987	0.974 to 0.993	1.8	2.0
	3	49.69	0.88	0.996	0.992 to 0.998	1.3	1.0
Distance from mitochondria to SR (nm)	1	6.10	1.00 [ref]	0.862	0.721 to 0.931	13.8	9.4
	2	4.45	0.73	0.944	0.892 to 0.972	9.4	7.3
	3	8.64	1.42	0.776	0.599 to 0.881	17.5	23.5
Mitochondria-SR interaction (%)	1	2.60	1.00 [ref]	0.943	0.860 to 0.974	4.5	4.5
	2	3.23	1.24	0.909	0.825 to 0.953	5.4	5.0
	3	5.92	2.27	0.763	0.544 to 0.879	6.8	7.5

Note: Rater 1, experienced rater; Rater 2 and 3, not experienced raters. n = 34 images.

Abbreviations: CI, confidence intervals; CV, coefficient of variability; SD, standard deviation.

TABLE 2 Reproducibility of measurements

Variable	Comparison	Limits of agreement method				Intraclass correlation		CV (%)	
		Bias	95% LoA	Slope	Intercept	Coefficient	95% CI	Mean	SD
Mitochondrial size (nm)	Rater 2 vs 1	72.07	−2.74 to 146.87	0.03	44.22	0.953	0.119 to 0.989	4.8	2.5
	Rater 3 vs 1	24.11	−104.26 to 152.47	0.07	−52.57	0.966	0.930 to 0.984	2.7	2.9
	Rater 3 vs 2	−47.96	−168.72 to 72.80	0.05	−98.73*	0.959	0.825 to 0.985	4.0	3.0
Distance from mitochondria to SR (nm)	Rater 2 vs 1	−0.41	−13.80 to 12.98	0.23	−3.44	0.428	0.105 to 0.668	29.2	32.0
	Rater 3 vs 1	3.86	−10.13 to 17.85	0.13	1.86	0.266	−0.035 to 0.537	30.4	24.7
	Rater 3 vs 2	4.27	−8.51 to 17.06	−0.11	5.84#	0.431	0.068 to 0.682	34.7	33.7
Mitochondria-SR interaction (%)	Rater 2 vs 1	1.00	−5.77 to 7.76	−0.03	1.43	0.613	0.356 to 0.785	11.3	11.8
	Rater 3 vs 1	3.48	-5.54 to 12.50	0.08	2.08	0.276	−0.047 to 0.555	18.2	14.1
	Rater 3 vs 2	2.48	−5.95 to 10.91	0.11	0.58	0.384	0.051 to 0.639	15.7	9.1

Note: Rater 1, experienced rater; Rater 2 and 3, not experienced raters. n = 34 images.

Abbreviations: 95% LoA, 95% limits of agreement; CI, confidence intervals; CV, coefficient of variability; SD, standard deviation.

#$P < .10$;

*$P < .05$ vs zero.

slopes and intercepts for these variables were not different from zero. Nevertheless, the ICCs were poor-to-moderate according to their 95% confidence intervals,[21] with CVs of ~30% for the distance from mitochondria to SR, and ~15% for the mitochondria-SR interaction. The images that generated the larger biases between raters were identified; those images are presented in Supporting Information Figure S2J-L, and their values are denoted with an arrow in Supporting Information Figure S2A-I.

3.3 | SM low Mfn2 protein abundance is accompanied by lower mitochondria-SR interaction and MIC60-MCD

The median value of Mfn2 protein in our sample distribution was used to split the subjects into Mfn2-HA and Mfn2-LA groups (Table 3). The metabolic and anthropometric parameters were similar between groups, except for LDL-C, which was higher in the Mfn2-LA group ($P = .003$; Table 3). There was also a trend for a higher age ($P = .09$) and BMI ($P = .07$) in the Mfn2-LA group (Table 3).

There were no differences in the protein levels of Mfn1 ($P = .24$) and Opa1 ($P = .18$) between groups (Figure 2A-D). Neither there were differences in mitochondrial size nor distance from mitochondria to the SR, either using the independent or the mean values from the three raters (Figure 2D,E,F,H,I,K,L,O). Nevertheless, the Mfn2-LA group had lower mitochondria-SR interaction as measured by the rater 1 ($P = .009$; Figure 2G) and the mean of the three raters ($P = .02$; Figure 2P); there was a similar trend when measured by the rater 2 ($P = .086$; Figure 2J). Only rater 3, did not detect a difference between groups in the mitochondria-SR interaction ($P = .94$; Figure 2M). No differences were found between groups in the percentage of

TABLE 3 Comparison between participants with high vs low Mfn 2 protein abundance in human SM

	HA-Mfn 2 (n = 6)	LA-Mfn 2 (n = 6)	*P* value
Age (y)	22.3 [3.6]	27.2 [5.7]	.09
BMI (Kg/m^2)	23.1 [2.1]	25.7 [2.6]	.07
Glucose (mg/dL)	84.2 [3.3]	89.7 [8.6]	.21
Insulin (μUL/mL)	6.1 [3.7]	11.9 [9.7]	.19
HOMA-IR	1.28 [0.8]	2.79 [2.7]	.18
LDL-C (mg/dL)	87.8 [22.4]	139.8 [24.3]	.009
HDL-C (mg/dL)	53.3 [17.3]	47.8 [9.5]	.77

Note: Values are mean [SD].

Abbreviations: BMI; body mass index; HDL-C, high-density lipoprotein cholesterol; HOMA-IR, homeostasis model assessment of insulin resistance; LDL-C, low-density lipoprotein cholesterol.

mitochondria-SR narrow (8-10 nm) or wide (40-50 nm) contact sites (Supporting Information Figure S3). No differences were found between groups in MCD (measured by stereological method; Supporting Information Figure S4; Figure 3A) when the mean of the individual MCD measurements was used ($P = .24$; Figure 3C); however, the Mfn2-LA group had a lower MCD when all mitochondria were integrated into the analyses, ($P = .03$; Figure 3D). In agreement, the Mfn2-LA group had a lower level of MIC60 ($P = .02$; Figure 3B-F), but not MIC19 protein ($P = .31$; Figure 3B-E). Additionally, we evaluated the protein level of mitochondrial oxidative phosphorylation (OXPHOS) complexes (Figure 3G-L), as this depends on the MCD, finding differences between groups only in the complex I ($P = .04$; Figure 3L) and tends in the complex IV ($P = .07$; Figure 3I). No differences were detected in SM fiber-type, as indicated by the Z-line width and mitochondrial

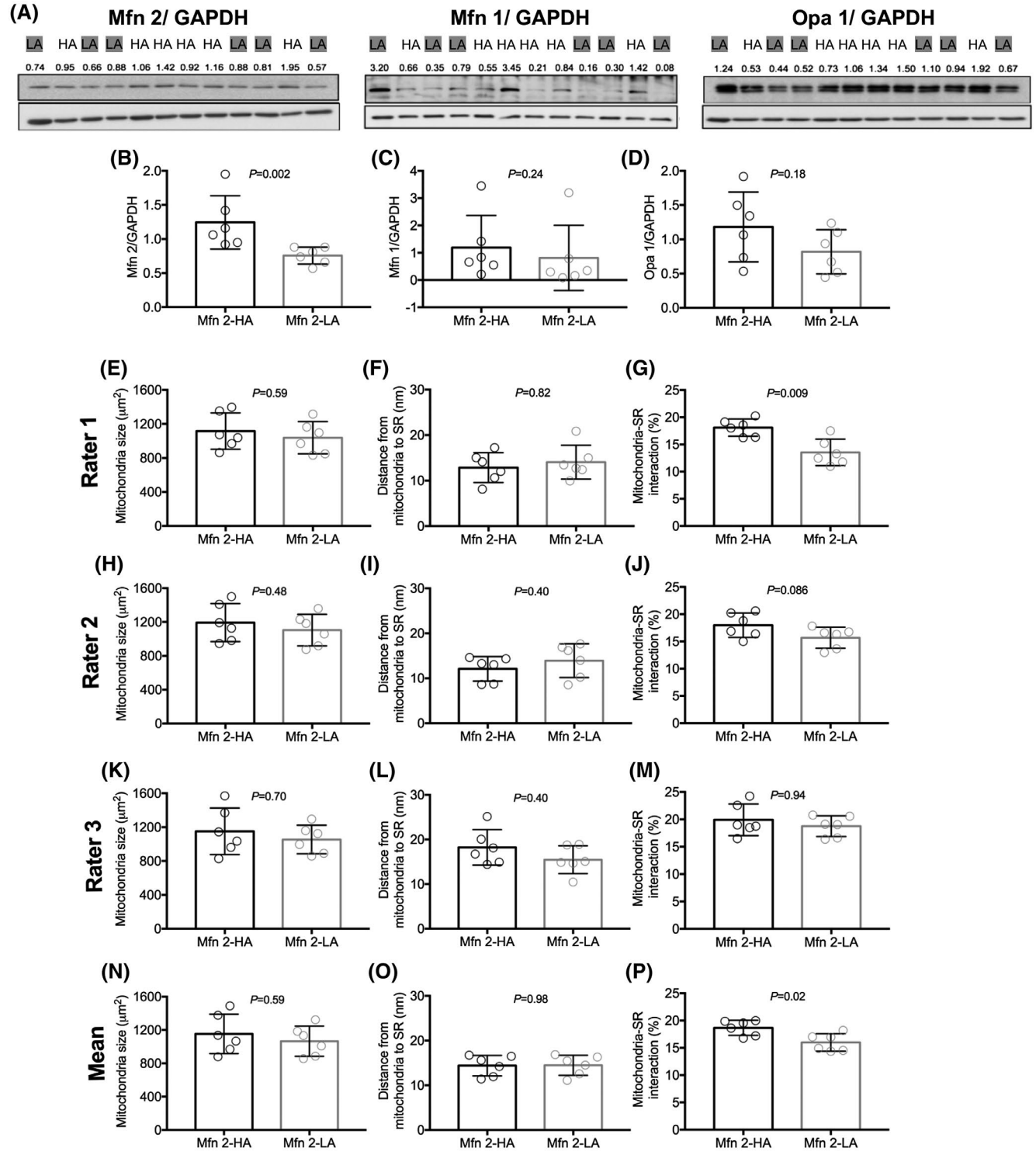

FIGURE 2 Potential role of skeletal muscle Mfn2 protein abundance on mitochondrial size and mitochondria-SR juxtaposition. Comparison between high vs low Mfn2 protein abundance groups (B) on Mfn1 (C) and Opa1 protein (D) (A; quantification of Western blot protein adjusted to GAPDH for each voluntary). Comparison between high vs low SM Mfn2 protein abundance groups on mitochondria size (E, H, K, N), distance from to SR (F, I, L, O), and mitochondrial-SR interaction (G, J, M, P) from TEM images. SR, sarcoplasmic reticulum; TEM, transition electron microscopy; SM, skeletal muscle; Mfn 2-HA, Mfn2-high abundance; Mfn 2-LA, Mfn2-low abundance

density (P = .98 and P = .13, respectively; Figure 4A-C). Nevertheless, the Mfn2-LA group had a lower VO_{2max} (P = .02; Figure 4D). Regarding SM quality, there were no differences in CSA (P = .48; Figure 5A-C) or MVC between groups (P = .93; Figure 5D). Finally, Mfn2 protein abundance was directly associated with mitochondria-SR interaction (mean of three raters) and MCD (P = .054; P = .037, respectively; Figure 6).

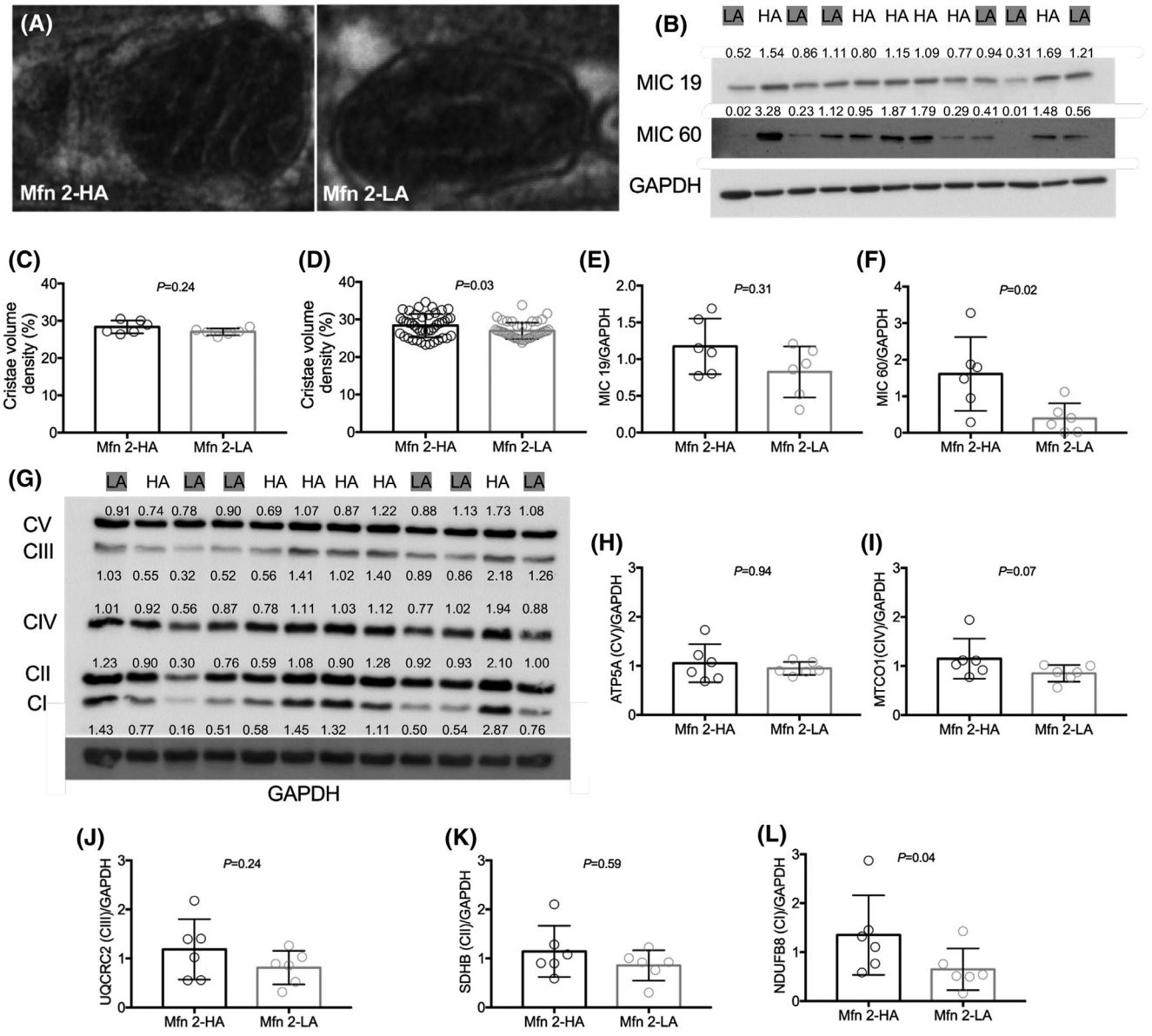

FIGURE 3 Potential role of skeletal muscle Mfn2 protein abundance on mitochondrial cristae density, MICOS proteins, and OXPHOS complexes. Representative images of mitochondrial cristae in human SM with Mfn 2-HA and Mfn 2-LA (A). Comparison between high vs low SM Mfn2 protein abundance groups on mitochondrial cristae density measured by stereological method (C [mean] - D [all mitochondria]), MICOS proteins (MIC60 and MIC19 [B, E-F; quantification of Western blot protein adjusted to GAPDH for each voluntary]), and proteins level of mitochondrial oxidative phosphorylation (OXPHOS) complexes in human SM (G-L; quantification of Western blot protein adjusted to GAPDH for each voluntary). SM, skeletal muscle; Mfn 2-HA, Mfn2-high abundance; Mfn 2-LA, Mfn2-low abundance

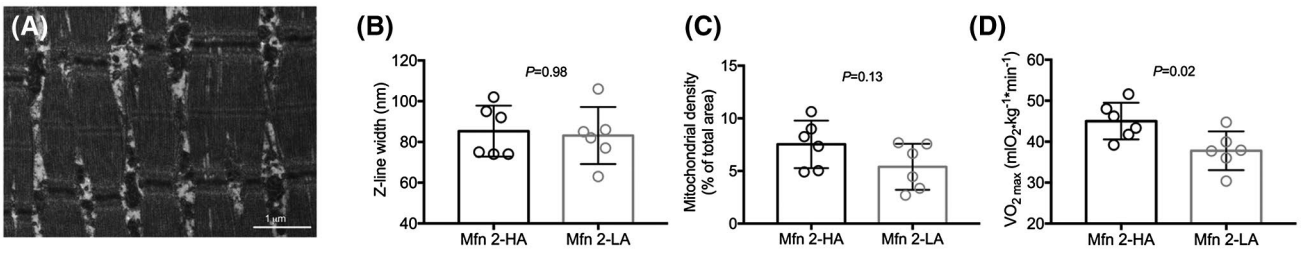

FIGURE 4 Potential role of skeletal muscle Mfn2 protein abundance on skeletal muscle fiber-type and maximal oxygen uptake. Comparison between high vs low Mfn2 protein abundance groups on SM fiber-type (A-C) and VO_{2max} (D). $VO_{2max,}$ maximal oxygen uptake; SM, skeletal muscle; Mfn 2-HA, Mfn2-high abundance; Mfn 2-LA, Mfn2-low abundance

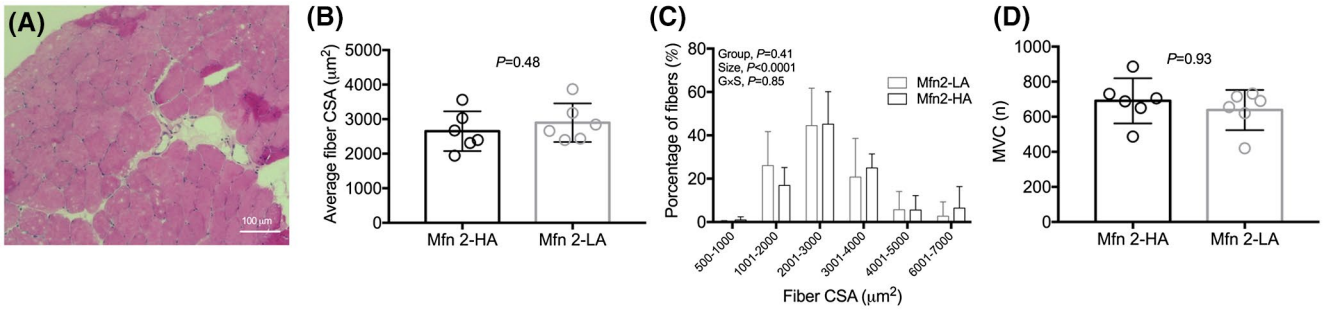

FIGURE 5 Potential role of skeletal muscle Mfn2 protein abundance on skeletal muscle quality. Comparison between high vs low SM Mfn2 protein abundance groups on CSA (A-C) and maximal strength (D). CSA, cross-sectional area; Mfn 2-HA, Mfn2-high abundance; Mfn 2-LA, Mfn2-low abundance

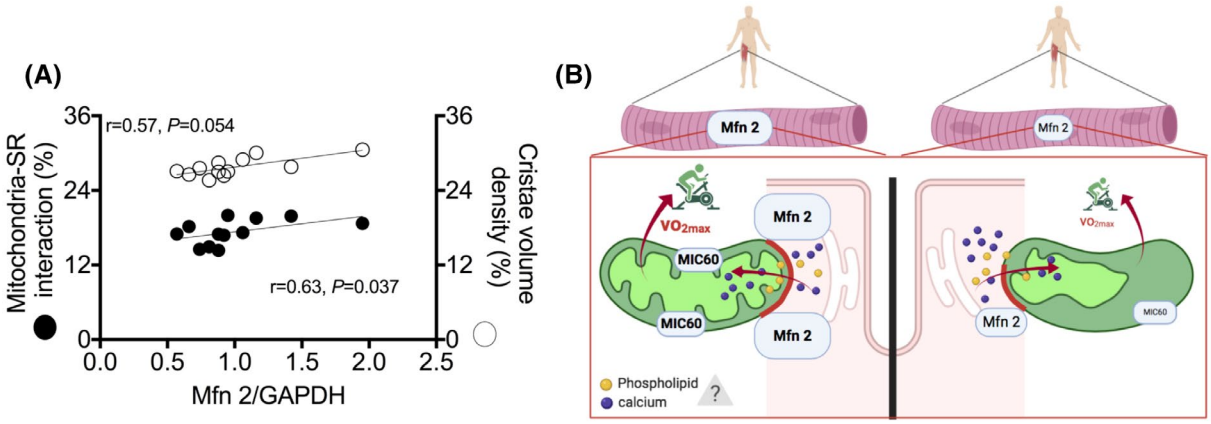

FIGURE 6 Skeletal muscle Mfn2 protein abundance is associated with mitochondria-SR interaction and mitochondrial cristae density. Spearman association between SM Mfn2 protein with mitochondria-SR interaction (mean three raters) and mitochondrial cristae density (A). Proposed model (B) created with BioRender.com

4 | DISCUSSION

The main findings of our study were that: (1) the measurement of mitochondrial size had high-to-excellent repeatability and—in general—a high reproducibility, whereas both parameters of mitochondria-SR juxtaposition (distance between organelles and percentage of mitochondria interacting with SR) had moderate repeatability, and a poor-to-moderate reproducibility; and (2) men healthy with low abundance of Mfn2 protein in SM had lower mitochondria-SR interaction and MCD compared to healthy subjects with a high abundance of Mfn2 protein, without differences in mitochondrial density. These results suggest that Mfn2 could play a role in the metabolic control of human men SM, by regulating the mitochondria-SR interaction.

4.1 | Repeatability and reproducibility

In SM, mitochondrial size is used as an index of fusion/fission phenotype, together with the measurement of proteins that regulate mitochondria fusion and fission. We showed that mitochondrial size—determined from TEM images—had high-to-excellent repeatability and high reproducibility. Notably, the mitochondria that generated the lowest repeatability and reproducibility were characterized by a large size and a blurred outer membrane.

Two important parameters to understand the interplay between mitochondria and SR are the distance and the interaction between these two organelles.[1,22] We observed that the bias between raters for the measurement of mitochondria-SR distance and mitochondria-SR interaction was ~4 nm and ~3.5%, respectively. In primary cortical neurons, increases in mitochondria-ER distance from ~25 to ~40 nm (aggregation of α-synuclein) were shown to reduce the basal respiration by ~35%.[22] In RBL-2H3 cells, decreases in mitochondrial-ER distance from ~24 to ~6 nm were reported to increase the mitochondrial calcium uptake by ~90%.[1] Similarly, a ~30% lower mitochondria-SR interaction surface area in SM was associated with decreased running exercise time in mice.[16] Furthermore, Mfn2-deficient murine cardiac myocyte was shown to decrease the mitochondria-SR interaction from ~48% to ~30%, leading to a 9% increase in caffeine-stimulated

cytosolic calcium release (transient amplitude).[15] Interestingly, all of these studies report shifts in mitochondria-ER/SR juxtaposition considerably higher than the bias between raters observed in the present study. Therefore, the measurement of mitochondria-SR distance and interaction from TEM images of human SM appears to be sensitive enough to detect the biologically relevant changes. We recommend, however, mitochondria-SR juxtaposition measurements to be carried out by experienced raters; as our data showed that the unexperienced rater did not have sensitivity enough to find the differences observed by the more experienced raters. Finally, we observed that the images that generated the lowest repeatability and reproducibility in the distance from mitochondria to SR and mitochondria-SR interaction are characterized by having an irregular SR morphology.

4.2 | Potential role of Mfn2 in mitochondria-SR juxtaposition, mitochondrial cristae, SM quality, and circulating blood markers

The role of Mfn2 on the regulation of mitochondria-SR/ER juxtaposition remains controversial.[12,13] Herein we observed that a lower abundance of Mfn2 in mature human SM was accompanied by a decreased mitochondrial-SR interaction. These results agree with animal work showing that the deletion of Mfn2 in the adult heart decreases the mitochondria-SR interaction.[23] We thus speculate that methodological and technical differences may explain the increased mitochondria-ER interaction observed after deletion of Mfn2 in certain studies. Another possibility is that Mfn2 has a cell- and stress-specific role in the regulation of mitochondrion-SR/ER juxtaposition.[24] For example, in neurons, the increase in Mfn2 was shown to decrease the mitochondrial-ER interaction.[24] That being said, our data support the evidence showing that deletion or a lower abundance of Mfn2 decreases the interaction between mitochondria and ER/SR.[2,4,7,8,10,13,15,23]

Mfn2 has been demonstrated to play a central role in the mitochondrial response to postprandial metabolic transitions in mice liver. Therein, Mfn2 couples the machineries that organize mitochondria-ER assembly and cristae architecture, which were previously thought to operate independently.[7] In agreement, we showed that the Mfn2-LA group had lower mitochondria-SR interaction and cristae density, accompanied by lower levels of MIC60 protein. MIC60 is the core component of the mitochondrial contact site and cristae organizing system and interacts with several inner and OMM proteins to maintain inner mitochondrial membrane morphology and density.[25] It has been suggested that the typical architecture of cristae provides a specific microenvironment that enhances the catalytic capacity of the OXPHOS system.[26] It was previously shown in HeLa cells that MIC60 knockout, decreases the activity of mitochondrial OXPHOS complexes I, III and IV.[27] Similarly, our results show that the Mfn2-LA group, which has low MIC60 protein, presents less mass of complex I and IV. We speculate that a higher abundance of Mfn2 leads to a greater mitochondria-SR interaction, facilitating calcium,[8] and/or lipid (phospholipid) transfer [28] from SR into the mitochondria, and increasing MCD through MIC60 (proposal model, Figure 6B). More studies are needed to elucidate the potential mechanism that regulates Mfn2 and MIC60 protein interaction.

The mitochondrion-SR interaction regulated by Mfn2 may also influence the formation of peroxisomes. In human fibroblasts, peroxisomes are formed by the fusion of mitochondria-derived vesicles with pre-peroxisomes derived from the SR.[29] The degree of mitochondria-SR interaction could thus either ease or limit the peroxisome formation. Interestingly, peroxisomes are currently recognized as essentials for metabolic health in skeletal muscle.[30,31] Future studies are, therefore, required to ascertain the role of mitochondria-SR interactions in peroxisome formation.

We showed that the Mfn2-LA group had a lower VO_{2max} (marker of mitochondrial function in human SM[32,33]), without differences in mitochondrial density (evaluated by TEM), mitochondrial size, and z-line width. These results support previous findings showing a direct association between SM Mfn2, but not Opa1 abundance and VO_{2peak} in obese and lean humans.[34] Regarding the role of Mfn2 abundance in SM quality, genetic deletion of Mfn2 was previously shown to decrease CSA and muscle strength.[9] In the present study, we did not find any association between Mfn2 abundance and CSA, muscle strength, or muscle fiber-type. Perhaps, the loss of the mitochondria-SR juxtaposition precedes the impairment in muscle quality in aging.[16] Finally, the differences in LDL-C between groups (higher in Mfn2-LA group) may represent the initial steps toward a disturbed lipid profile mediated by decreases in Mfn2 protein in SM. This could result from a reduced tissular capacity to adapt fuel oxidation to fuel availability, that is, an impaired metabolic flexibility.[35] We have recently shown that healthy subjects with low metabolic flexibility have higher circulating LDL-C than subjects with high metabolic flexibility.[36] Impaired metabolic flexibility has been also related to muscle insulin resistance and other metabolic disturbances.[35,37] Notably, metabolic flexibility was previously shown to associate directly with Mfn2 expression in human SM,[38] thus suggesting a link between SM Mfn2 protein abundance, metabolic flexibility, and metabolic health. Future studies should evaluate whether SM Mfn2-LA is a risk factor in the weight gain induced by hypercaloric diets in humans.

A limitation of the present study was that we only used conventional TEM images to measure the mitochondria-SR juxtaposition. Additional measurements using immune-gold staining or 3D-electron tomography to determine mitochondria-SR juxtaposition would have strengthened the current findings. In conclusion, we have shown that the measurement of mitochondrial size has high-to-excellent repeatability and reproducibility; however, the repeatability and reproducibility

of mitochondrial-SR juxtaposition measurement was poor-to-moderate. As expected, the raters with the highest experience showed better repeatability and reproducibility. We thus recommend mitochondria-SR juxtaposition to be measured by experienced raters to obtain reproducible results. Furthermore, we have shown that low Mfn2 protein abundance associates with a reduced interaction mitochondria-SR, MIC 60 protein-MCD, and VO_{2max}, along with disturbances in lipid metabolism. This suggests that Mfn2 protein abundance plays a role in the metabolic control of human men SM.

ACKNOWLEDGMENTS

Thanks to all participants, to Daniela Avalos and German Tapia for your technical assistance. This work was supported by the Unidad de Microscopía Avanzada UC (UMA UC). We also extend our thanks to Dr. Graham P. Holloway for providing insight into manuscript, and Dr. Matias Monsalves for providing MIC60 and MIC19 antibodies.

DISCLOSURES

No conflict of interest, financial or otherwise, are declared by the authors.

AUTHOR CONTRIBUTIONS

M. Castro-Sepulveda conceived and designed research; M. Castro-Sepulveda, M. Troncoso and S. Jannas-Vela performed experiments; M. Castro-Sepulveda, R. Fernández-Verdejo, M. Tuñón-Suárez, J. Morales-Zúñiga, and S. Jannas-Vela analyzed the data; M. Castro-Sepulveda and R. Fernández-Verdejo prepared figures; M. Castro-Sepulveda, R. Fernández-Verdejo, S. Jannas-Vela, and H. Zbinden-Foncea drafted the manuscript; All authors approved the final version of manuscript.

REFERENCES

1. Csordás G, Renken C, Várnai P, et al. Structural and functional features and significance of the physical linkage between ER and mitochondria. *J Cell Biol*. 2006;174(7):915-921.
2. Csordás G, Weaver D, Hajnóczky G. Endoplasmic reticulum-mitochondrial contactology: structure and signaling functions. *Trends Cell Biol*. 2018;28(7):523-540.
3. Eisner V, Csordás G, Hajnóczky G. Interactions between sarco-endoplasmic reticulum and mitochondria in cardiac and skeletal muscle—pivotal roles in Ca^{2+} and reactive oxygen species signaling. *J Cell Sci*. 2013;126(14):2965-2978.
4. de Brito OM, Scorrano L. Mitofusin 2 tethers endoplasmic reticulum to mitochondria. *Nature*. 2008;456(7222):605-610.
5. Filadi R, Greotti E, Turacchio G, et al. Mitofusin 2 ablation increases endoplasmic reticulum-mitochondria coupling. *Proc Natl Acad Sci U S A*. 2015;112(17):E2174-E2181.
6. Filadi R, Pendin D, Pizzo P. Mitofusin 2: from functions to disease. *Cell Death Dis*. 2018;9(3):330.
7. Sood A, Jeyaraju DV, Prudent J, et al. A Mitofusin-2-dependent inactivating cleavage of Opa1 links changes in mitochondria cristae and ER contacts in the postprandial liver. *Proc Natl Acad Sci U S A*. 2014;111(45):16017-16022.
8. Ainbinder A, Boncompagni S, Protasi F, Dirksen RT. Role of Mitofusin-2 in mitochondrial localization and calcium uptake in skeletal muscle. *Cell Calcium*. 2015;57(1):14-24.
9. Sebastián D, Sorianello E, Segalés J, et al. Mfn2 deficiency links age-related sarcopenia and impaired autophagy to activation of an adaptive mitophagy pathway. *EMBO J*. 2016;35(15):1677-1693.
10. Tubbs E, Chanon S, Robert M, et al. Disruption of mitochondria-associated endoplasmic reticulum membrane (MAM) integrity contributes to muscle insulin resistance in mice and humans. *Diabetes*. 2018;67(4):636-650.
11. Castro-Sepulveda M, Jannas-Vela S, Fernández-Verdejo R, et al. Relative lipid oxidation associates directly with mitochondrial fusion phenotype and mitochondria-sarcoplasmic reticulum interactions in human skeletal muscle. *Am J Physiol Endocrinol Metab*. 2020;318(6):E848-E855.
12. Filadi R, Greotti E, Turacchio G, et al. On the role of Mitofusin 2 in endoplasmic reticulum-mitochondria tethering. *Proc Natl Acad Sci U S A*. 2017;114(12):E2266-E2267.
13. Naon D, Zaninello M, Giacomello M, et al. Critical reappraisal confirms that Mitofusin 2 is an endoplasmic reticulum-mitochondria tether. *Proc Natl Acad Sci U S A*. 2016;113(40):11249-11254.
14. Cieri D, Vicario M, Giacomello M, et al. SPLICS: a split green fluorescent protein-based contact site sensor for narrow and wide heterotypic organelle juxtaposition. *Cell Death Differ*. 2018;25(6):1131-1145.
15. Chen Y, Csordás G, Jowdy C, et al. Mitofusin 2-containing mitochondrial-reticular microdomains direct rapid cardiomyocyte bioenergetic responses via interorganelle Ca(2+) crosstalk. *Circ Res*. 2012;111(7):863-875.
16. Del Campo A, Contreras-Hernández I, Castro-Sepúlveda M, et al. Muscle function decline and mitochondria changes in middle age precede sarcopenia in mice. *Aging*. 2018;10(1):34-55.
17. Nielsen J, Gejl KD, Hey-Mogensen M, et al. Plasticity in mitochondrial cristae density allows metabolic capacity modulation in human skeletal muscle. *J Physiol*. 2017;595(9):2839-2847.
18. Kelley DE, He J, Menshikova EV, Ritov VB. Dysfunction of mitochondria in human skeletal muscle in type 2 diabetes. *Diabetes*. 2002;51(10):2944-2950.
19. Peñailillo L, Aedo C, Cartagena M, et al. Effects of eccentric cycling performed at long vs. short muscle lengths on heart rate, rate perceived effort, and muscle damage markers. *J Strength Cond Res*. 2020;34(10):2895-2902.
20. Bland JM, Altman DG. Measuring agreement in method comparison studies. *Stat Methods Med Res*. 1999;8(2):135-160.
21. Koo TK, Li MY. A guideline of selecting and reporting intraclass correlation coefficients for reliability research. *J Chiropr Med*. 2016;15(2):155-163.
22. Faustini G, Marchesan E, Zonta L, et al. Alpha-synuclein preserves mitochondrial fusion and function in neuronal cells. *Oxid Med Cell Longev*. 2019;23:4246350.
23. Beikoghli Kalkhoran S, Hall AR, White IJ, et al. Assessing the effects of mitofusin 2 deficiency in the adult heart using 3D electron tomography. *Physiol Rep*. 2017;5(17):e13437.
24. Puri R, Cheng X-T, Lin M-Y, et al. Mul1 restrains Parkin-mediated mitophagy in mature neurons by maintaining ER-mitochondrial contacts. *Nat Commun*. 2019;10(1):3645.
25. von der Malsburg K, Müller J, Bohnert M, et al. Dual role of mitofilin in mitochondrial membrane organization and protein biogenesis. *Dev Cell*. 2011;21(4):694-707.
26. Echeverria F, Jimenez Patino PA, Castro-Sepulveda M, et al. Microencapsulated pomegranate peel extract induces mitochondrial complex IV activity and prevents mitochondrial cristae

alteration in brown adipose tissue in mice fed on a high-fat diet. *Br J Nutr*. 2020;1-12.
27. Yang R-F, Sun L-H, Zhang R, et al. Suppression of Mic60 compromises mitochondrial transcription and oxidative phosphorylation. *Sci Rep*. 2015;5:7990.
28. Hernández-Alvarez MI, Sebastián D, Vives S, et al. Deficient endoplasmic reticulum-mitochondrial phosphatidylserine transfer causes liver disease. *Cell*. 2019;177(4):881-895.e17.
29. Sugiura A, Mattie S, Prudent J, McBride HM. Newly born peroxisomes are a hybrid of mitochondrial and ER-derived pre-peroxisomes. *Nature*. 2017;542(7640):251-254.
30. Huang T-Y, Zheng D, Hickner RC, et al. Peroxisomal gene and protein expression increase in response to a high-lipid challenge in human skeletal muscle. *Metabolism*. 2019;98:53-61.
31. Noland RC, Woodlief TL, Whitfield BR, et al. Peroxisomal-mitochondrial oxidation in a rodent model of obesity-associated insulin resistance. *Am J Physiol Endocrinol Metab*. 2007;293(4):E986-E1001.
32. Jacobs RA, Lundby C. Mitochondria express enhanced quality as well as quantity in association with aerobic fitness across recreationally active individuals up to elite athletes. *J Appl Physiol*. 2013;114(3):344-350.
33. Distefano G, Standley RA, Dubé JJ, et al. Chronological age does not influence ex-vivo mitochondrial respiration and quality control in skeletal muscle. *J Gerontol A Biol Sci Med Sci*. 2017;72(4):535-542.
34. Arribat Y, Broskey NT, Greggio C, et al. Distinct patterns of skeletal muscle mitochondria fusion, fission and mitophagy upon duration of exercise training. *Acta Physiol*. 2019;225(2):e13179.
35. Galgani JE, Fernández-Verdejo R. Pathophysiological role of metabolic flexibility on metabolic health. *Obes Rev*. 2021;22(2):e13131.
36. Fernández-Verdejo R, Castro-Sepulveda M, Gutiérrez-Pino J, et al. Direct relationship between metabolic flexibility measured during glucose clamp and prolonged fast in men. *Obesity*. 2020;28(6):1110-1116.
37. Fernández-Verdejo R, Bajpeyi S, Ravussin E, Galgani JE. Metabolic flexibility to lipid availability during exercise is enhanced in individuals with high insulin sensitivity. *Am J Physiol Endocrinol Metab*. 2018;315(4):E715-E722.
38. Mingrone G, Manco M, Calvani M, et al. Could the low level of expression of the gene encoding skeletal muscle mitofusin-2 account for the metabolic inflexibility of obesity? *Diabetologia*. 2005;48(10):2108-2114.

SUPPORTING INFORMATION

Additional Supporting Information may be found online in the Supporting Information section.

How to cite this article: Castro-Sepulveda M, Fernández-Verdejo R, Tuñón-Suárez M, et al. Low abundance of Mfn2 protein correlates with reduced mitochondria-SR juxtaposition and mitochondrial cristae density in human men skeletal muscle: Examining organelle measurements from TEM images. *The FASEB Journal*. 2021;35:e21553. https://doi.org/10.1096/fj.202002615RR